Modelling of the constitutive behaviour of welded structural panels made of 2198-T8 aluminium alloy

Xavier TRUANT, Georges CAILLETAUD**, Florent FOURNIER DIT CHABERT* and Serge KRUCH**
**ONERA, 29 Av. Division Leclerc, B.P.72, 92322 Châtillon Cedex, France*
xavier.truant@onera.fr
***Centre des Matériaux, MINES ParisTech, CNRS UMR 7633, 10 rue Henri Desbruères, B.P. 87, 91003 Evry Cedex, France*

Abstract

The Friction Stir Welding (FSW) process generally induces a critical hardness decrease inside the welded joint. To design aeronautical structure welded by FSW, it is then necessary to know the impact of this hardness drop on the constitutive behaviour of the junction. In this study, the hardening structural aluminium alloy 2198-T8 is considered. Many monotonic and cyclic mechanical tests were carried out. Digital Image Correlation (DIC) is used to measure local displacement fields around the junction. Finally, based on this experimental data, a constitutive model is proposed and identified for the welded joint.

1. Introduction

The FSW process was developed in 1991 by The Welding Institute [1]. The FSW is a solid state process without any filler material. Temperatures reached are lower than the melting temperature of the material. This enables the welding of hard weldable materials such as aluminium alloys of the 2XXX serie [2]. Nowadays, it is used in the aeronautical field as an alternative of the riveting process. The third generation aluminium alloy 2198-T8 is considered in this study. The addition of lithium enhances the mechanical properties compared to 2024 [3] and reduces the weight of structures. ONERA has carried out many works on the influence of the process parameters on the microstructure and tensile properties of the welding joint. The aim of this study is to develop a constitutive model of welded joints tested under complex multiaxial loadings.

2. Experimental study of the mechanical behaviour of the welded joints

2.1 Welding of the samples

FSW was carried out at the ONERA with a Crawford Swift Ltd POWERSTIR 25T machine, using an advancing on rotational speed of 0.4. The tool used [4] has a shoulder diameter of 13 mm and a pine diameter of 4.2 mm. The pine length is adjusted for being smaller than the sheet metal thickness which is around 3.18 mm. Welding was mainly performed along the longitudinal rolling direction called L. Nevertheless, as the 2198-T8 material is known to be strongly anisotropic, welding was also performed along the 2 other main directions of rolling (called T for the transverse one and D for the 45° direction). It is very important to study the effect of the welding direction versus the rolling direction of the sheet on the mechanical properties of the welded joints. In this paper, only results on the welding direction along the L axis are presented. Results along T and D axes are in progress.

2.2 Mechanical tests

Monotonic tensile tests and cyclic tests were carried out at room temperature on a 100 kN servohydraulic LOS SYSTEM Losenhausen (Great Britain) Ltd machine. Cyclic tests were performed on the same facility with a symmetrical loading ratio ($R = \sigma_{min}/\sigma_{max} = -1$). An anti-buckling device has been designed as proposed by Khan and co [5]. For each sample, 4 successive levels of load were tested (Figure 1). Both the base metal and the welded joints were tested using either strain or stress control.

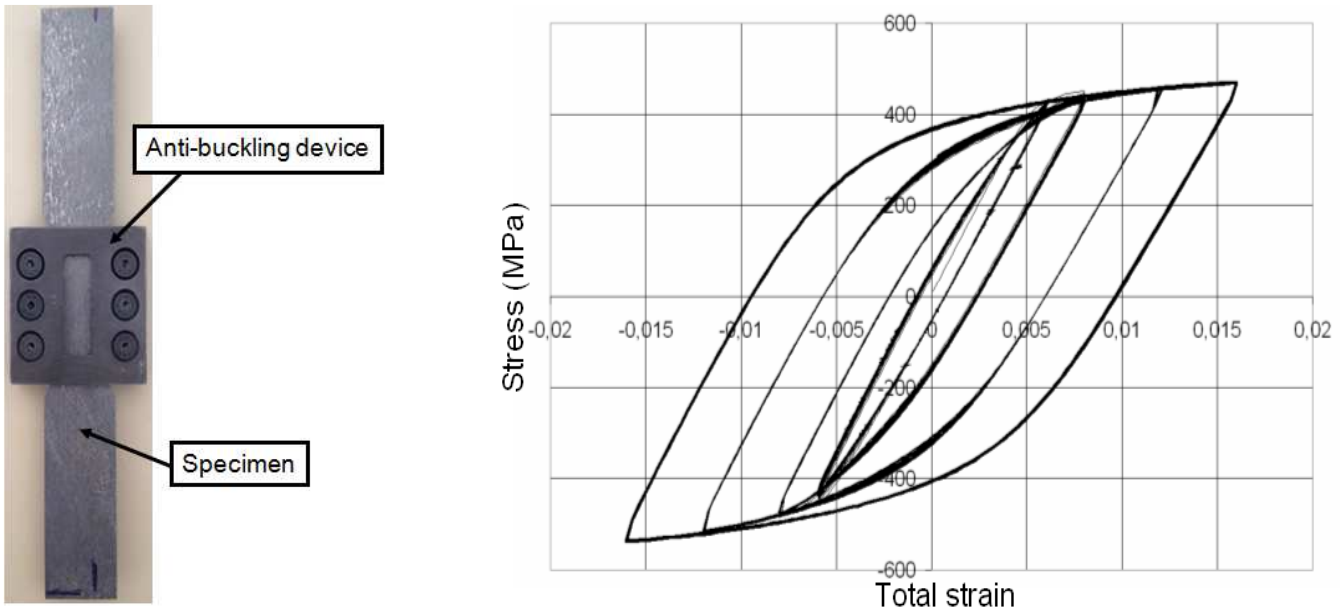

Figure 1: Anti-buckling device and the base metal specimen (left), global mechanical behaviour of the base metal for symmetric loadings and four different strain levels (right)

For the welded samples, Digital Image Correlation (DIC) has been used to mesure the displacement fields and thus to obtain the local stress-strain curves. This technique has already been used on inhomogeneous materials [6]. During mechanical tests, pictures are taken using a camera Aramis 4M, CMOS, Titanar 5.6/100 (resolution 2352x1728 pixels). The grey level contrast is obtained using a speckle pattern at the sample surface made of black and white paintings. The ARAMIS software [7] was used to analyse the pictures, to measure the displacement fields and finally to calculate the strain fields. For the DIC, image subsets of 35x35 pixels were chosen which corresponds to a 0.6x0.6 mm area. Such dimension of subsets is well suitable to catch the gradient of the mechanical properties across the welded joint with a quite good accuracy.

2.3 Experimental results

Figure 2 shows some results of strain fields at three different times during the tensile test. Figure 3 is a graph of the displacement as a function of the position along the loading axis and the strain at these same positions, at t=16.97s and t=40.40s (Images 1 and 3, in Figure 2). At the beginning of the tensile test, the displacement curve is linear across the welding joint. Experimental displacement data are evenly spaced and strain is homogeneous inside the sample. At the end of the tensile test, the shape of the displacement curve describes a sigmoidal curve. The displacement contours are no longer evenly spaced. The strain in the region in and near the weld varies from approximately 0.4% outside the shoulder diameter to near 30% in the nugget centre. The weld creates a strong inhomogeneity in material properties and the bulk of the plastic deformation is concentrated in the weld region. To sum up, strain is localized in the weakest zone of the sample which is, in our case, the weld centreline (Images 2 and 3, Figure 2). The local DIC assessed stress-strain response in the centre of the weldment shows a strong level of plasticity whereas the base metal remains mainly elastic.

Constitutive stress-strain behaviour can be directly extracted from localized regions in the DIC results. For example, local strain value can be compared to strain values recorded by a macroscopic extensometer (Figure 4a). For this analysis, the stress was assumed to be the continuum engineering stress value at all locations in the field. These results validate that the DIC method assesses strain values that are identical to those obtained by conventional methods. Then, the local strain values can be assessed in other regions from the centreline of the joint (red curve in Figure 4b) to the base metal (black curve in Figure 4b). As discussed before, the centre of the weldment shows a strong level of plasticity whereas the base metal remains practically elastic. From a constitutive behaviour point of view, the weld appears to have a lower yield strength and a higher hardening module than the base metal.

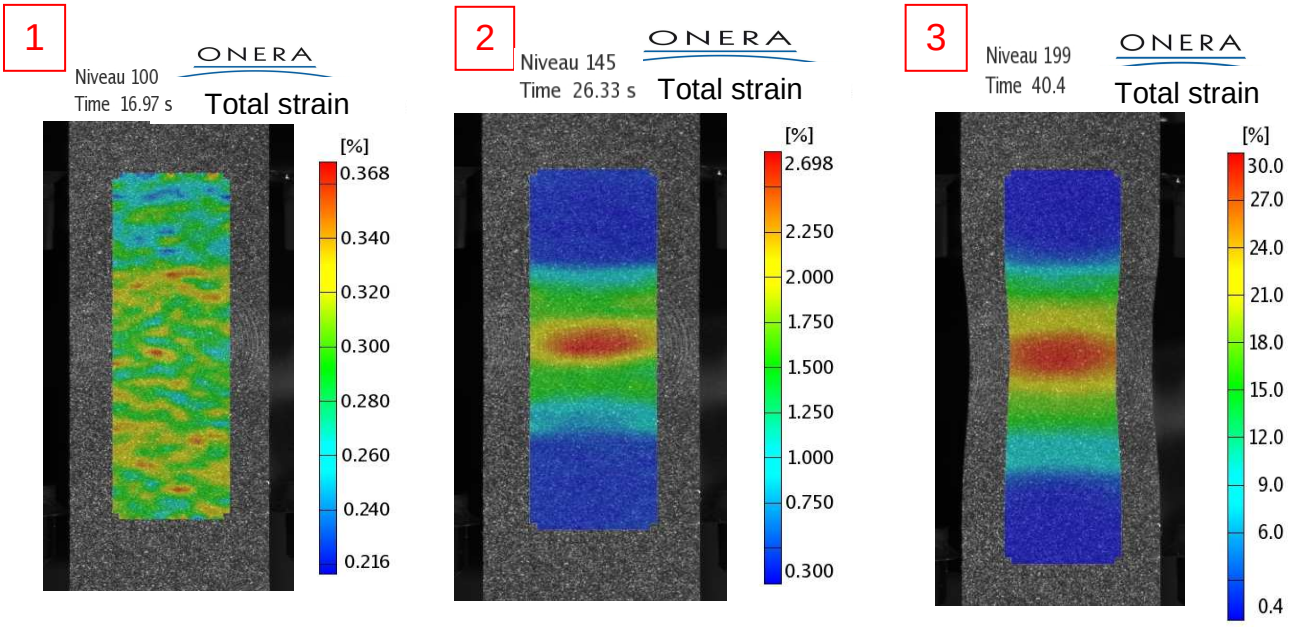

Figure 2: Results of strain fields at six different times during the tensile test

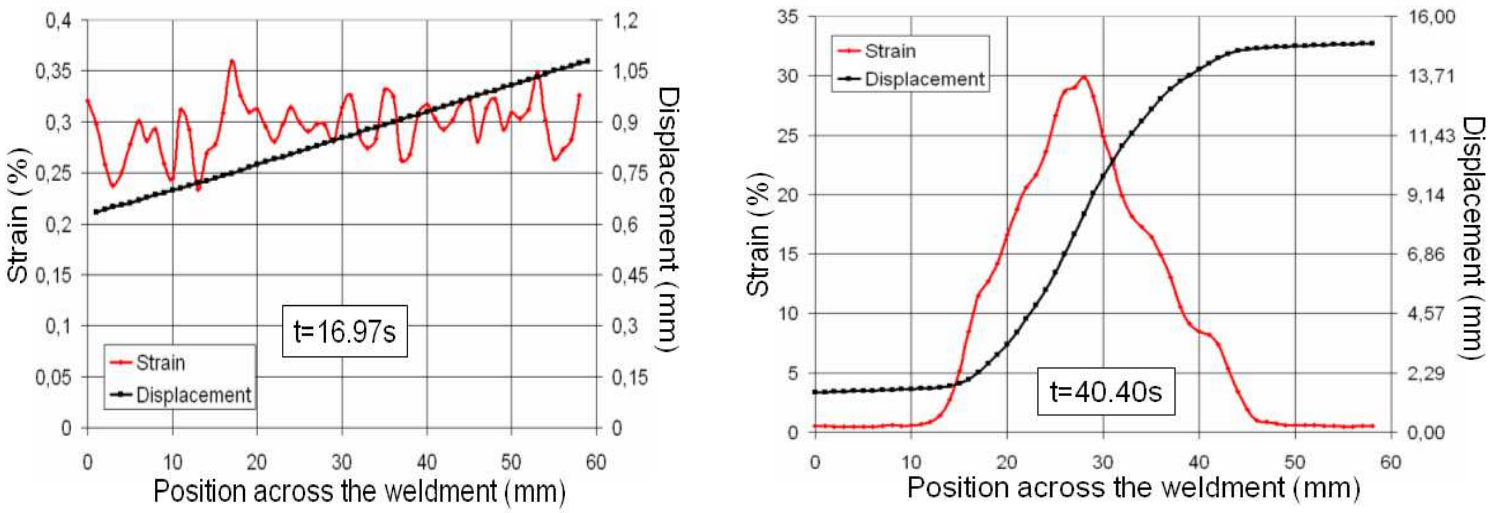

Figure 3: Evolution of the displacement as a function of the position along the loading axis and the strain at these same positions, at t=16.97s and t=40.40s

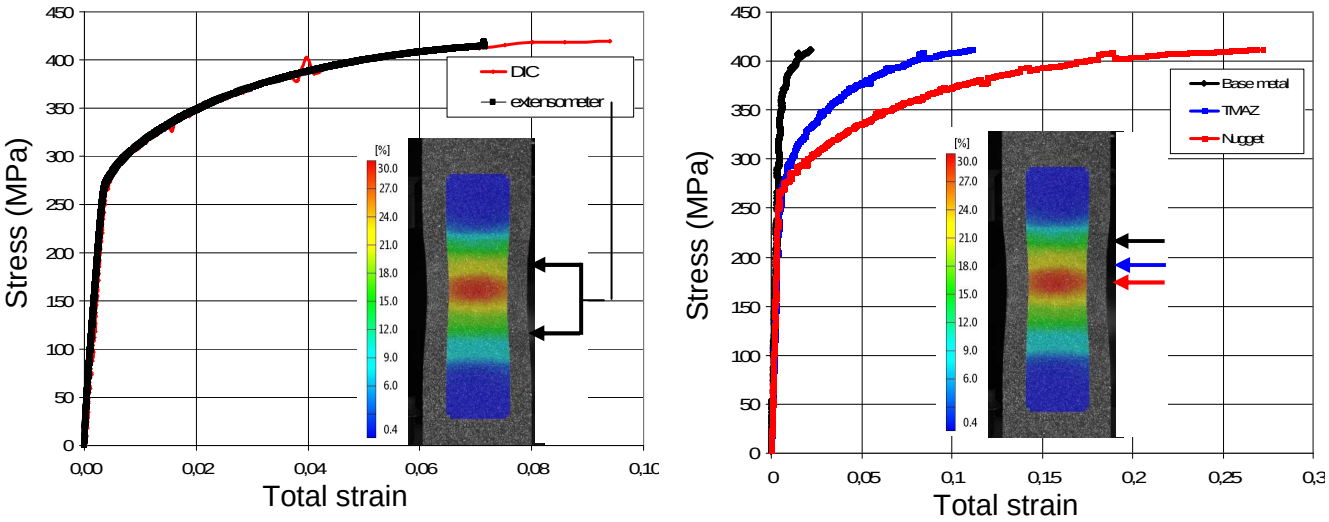

Figure 4: a) Comparison between the DIC assessed strain values and those obtained by conventional method, b) Assessment of the local strain values at 3 different regions of the welded joint

The experimental device being well set up, complex cyclic tests have been carried out to characterise the local cyclic mechanical behaviour of the welded joint. Figure 5 shows the constitutive stress-strain behaviour of the nugget zone directly extracted from the DIC results. Again, the stress was assumed to be the continuum engineering stress value in each section of the specimen. For each stress level, only the first hysteresis loop is plotted to facilitate the reading of the figure. As observed before, the nugget area shows a strong level of plasticity. An important isotropic hardening is also observed in each zone of the welded joint. The evolution of the total plastic range with the number of cycles is shown on Figure 6. The nugget zone exhibits a higher isotropic hardening than the others regions. We can notice that the number of cycles performed is not enough to reach the stabilized hysteresis loop. These results will be improved on longer cyclic tests.

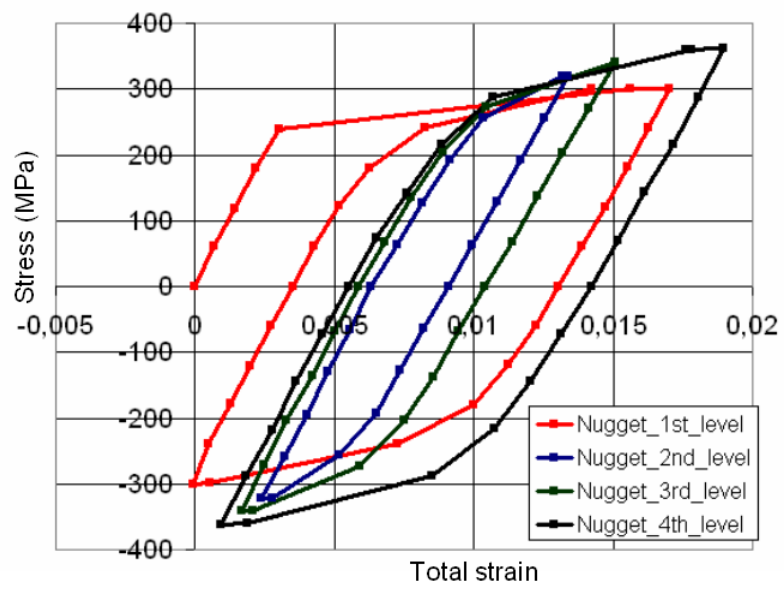

Figure 5: Local behaviour of the nugget zone got with DIC for symmetric loadings

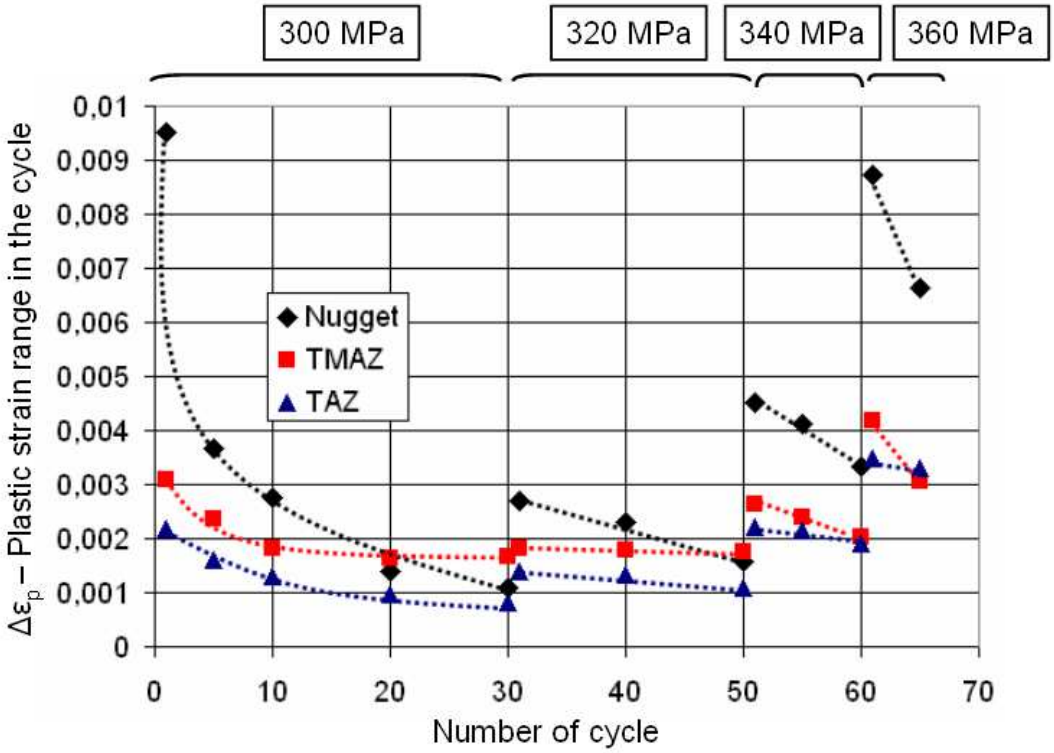

Figure 6: Observation of hardening for three different zones in the welded joint and for four stress levels

These results validate the DIC method in order to assess constitutive stress-strain behaviour directly extracted from localized regions in the experimental sample. In particular, kinematic and isotropic hardenings can be clearly identified. However, the strain range, over which the constitutive behaviour of a particular region of the weld is measured, is limited by the strength of the weakest zone of the weld microstructure. Tensile test results show that, just before the rupture of the specimen, base metal exhibits quite low plasticity whereas the centreline of the weld exhibits a strong level of plasticity. Hence, assessment of the cyclic constitutive behaviour of the base metal needs to be performed on homogeneous specimens without welds.

3. Model identification

Aluminium sheets are strongly non isotropic as a result of the rolling process. Nonetheless, as we consider, for the moment, samples with the welding direction along the L rolling direction, we decided to use, as a first approximation, an isotropic elasto-viscoplastic Chaboche model. For the uniaxial case, equations are briefly presented below. The viscoplastic potential contains a plasticity threshold R_0, 2 non- linear isotropic hardenings R_i and 3 nonlinear kinematic hardenings (X_1, X_2 and X_3).

$$\dot{\varepsilon}^p = \left\langle \frac{\sigma - X - R}{K} \right\rangle^n$$

$$X = X_1 + X_2 + X_3$$

$$dX_i = C_i \, d\varepsilon^p - D_i \, X_i \left| d\varepsilon^p \right|$$

$$R = R_0 + \sum_i^2 Q_i (1 - \exp(-b_i \, p))$$

$$dR_i = b_i (Q_i - R_i) dp$$

The result of the identification of the parameters of the model is given for the nugget (Table 1). Results are shown on Figure 7. A quite good agreement is obtained. A similar work has been done for nine other zones across the welding joint. Zones have been chosen in order to reproduce precisely the gradient of the mechanical behaviour experimentally observed.

Table 1: Identification of mechanical parameters

Young Modulus	Plasticity threshold	Non Linear Isotropic Hardening 1		NLIH 2		Non Linear Kinematic Hardening 1		NLKH 2		NLKH 3		Viscosity potential	
E (GPa)	σ_y (MPa)	b1	Q1 (MPa)	b2	Q2	C1 (MPa)	D1	C2	D2	C3	D3	n	K
81	255	400	-105	17	130	40000	4500	50000	450	1700	100	17	600

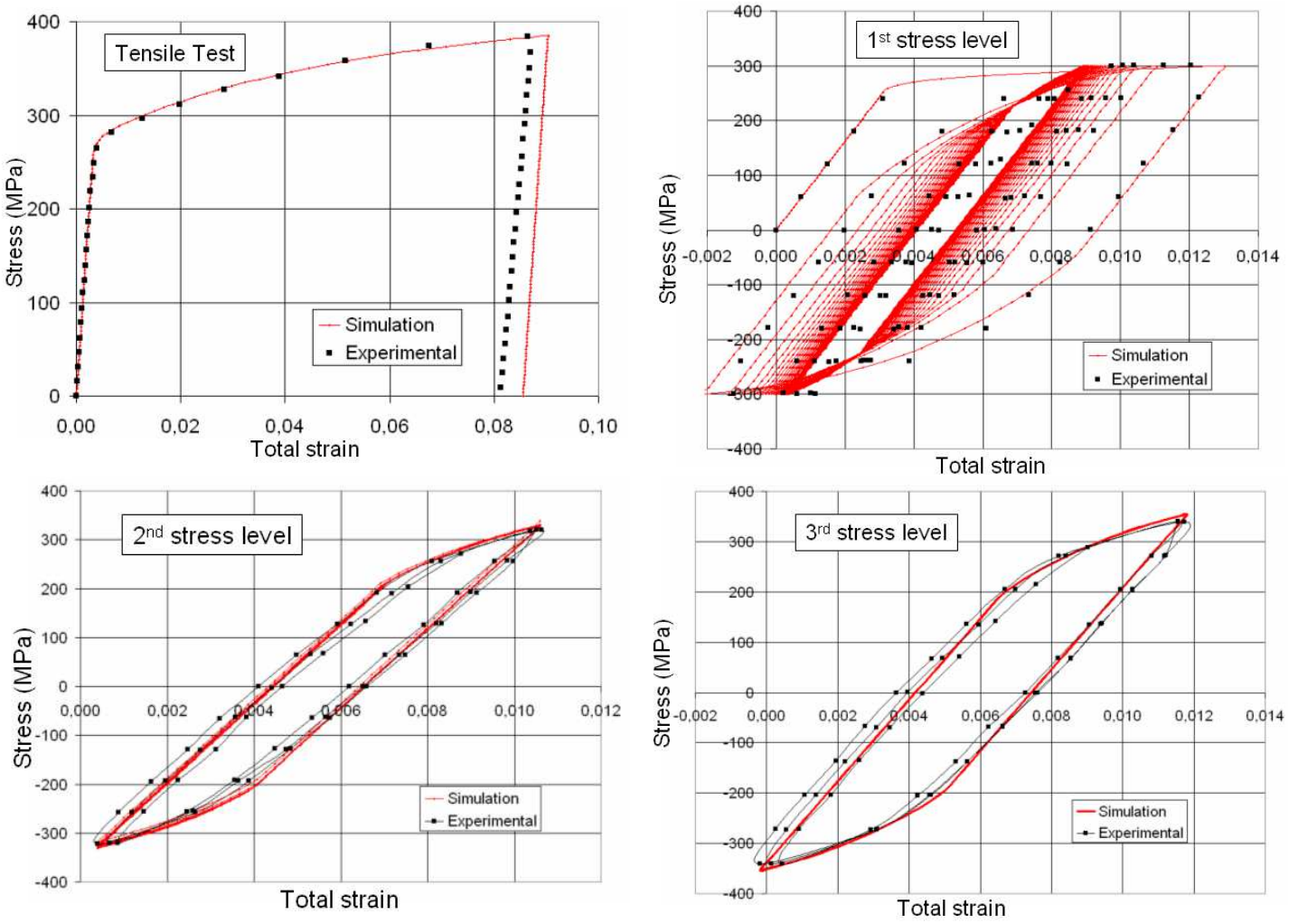

Figure 7: Comparison between simulation and experimental results for a tensile test (upper left corner) and for a cyclic test with symmetric loadings and three different stress levels

4. Multiaxial loadings

A more complex test has been proposed in order to observe the cyclic behaviour of the welded joint and to validate the proposed model under multiaxial loads. For this purpose a cruciform specimen has been designed in order to impose tension/tension loads (Figure 8). The test was performed with loadings of 150 kN on the axis perpendicular to the welded joint and 15 kN on the other one. Figure 9 shows a comparison between the numerical simulation and the experimental result.
The isotropic model presented before, gives a good agreement with the experimental result obtained with the DIC method. However, for more important loadings in the axis of the joint, it is possible the anisotropic effects of the material should be taken in account.

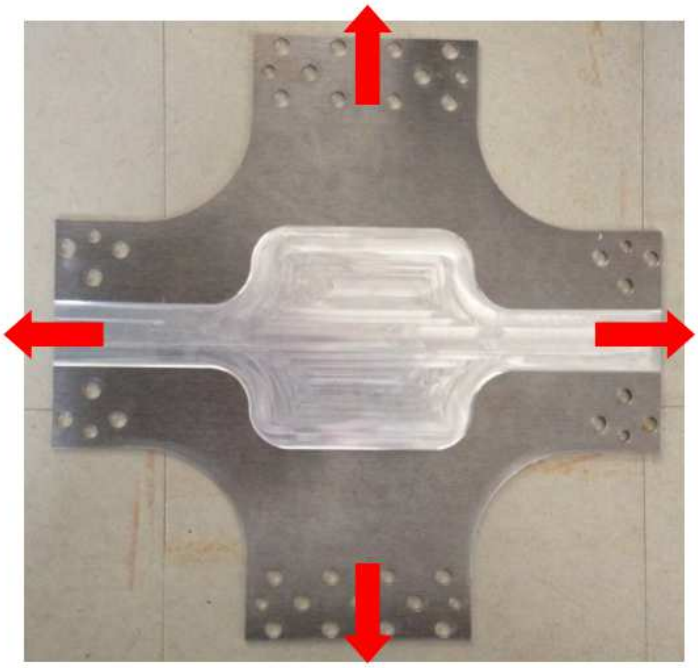

Figure 8: Design of a cruciform specimen

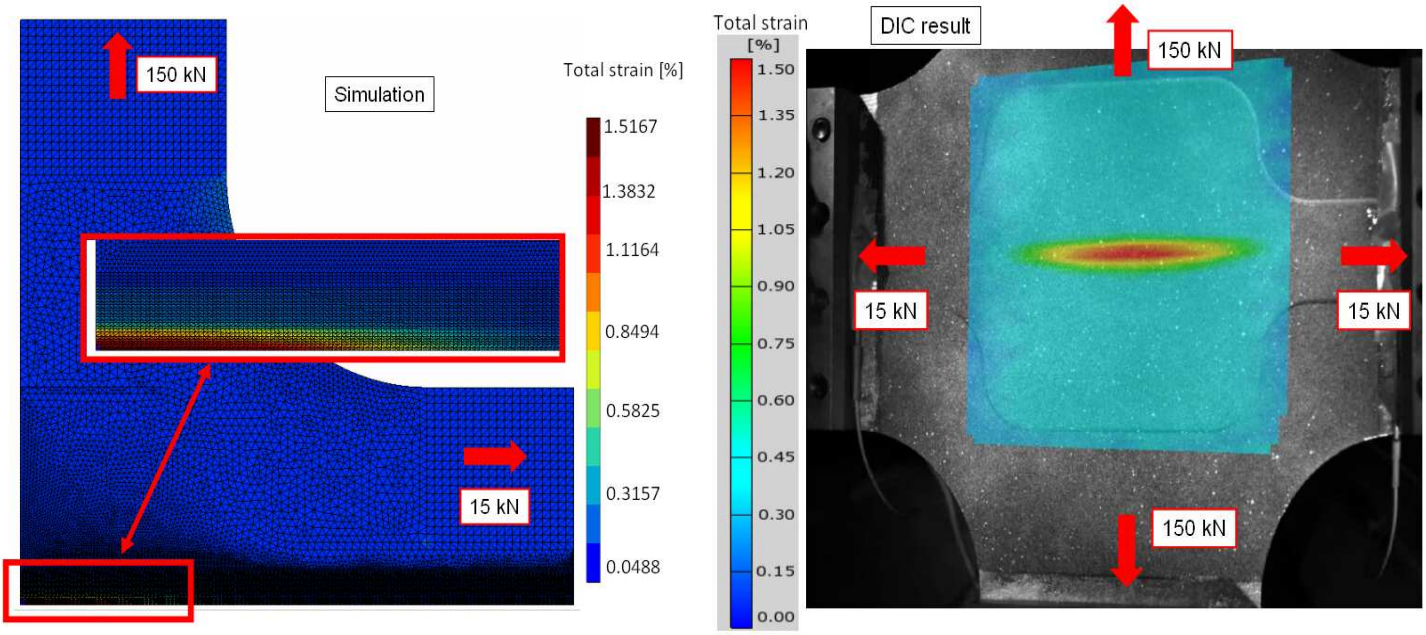

Figure 9: Comparison between the numerical simulation and the experimental result for a multiaxial loading test (150 and 15 kN)

5. Conclusion

This study focuses on 2198-T8 metal sheet welded by FSW. Microstructural analysis of welded joints coupled with hardness measurements performed crosswise to the weldment showed some important changes due to the FSW process. 3.18mm thick transverse specimens were machined from the welds and mechanically tested with the welding direction perpendicular to loading direction. Tensile and cyclic tests were performed at ambient temperature. DIC results validate that this technique is able to assess the constitutive stress-strain behaviour gradient of the welded joint. In a first step to model such mechanical gradient, an isotropic constitutive model for the welded joint has been proposed. A multiaxial test was carried out in order to validate this model. Finally, to improve the simulation results, an anisotropic model will be proposed.

References

[1] W. Thomas. 1991. www.twi-global.com. TWI.

[2] Rajiv S. Mishra, Murray W. Mahoney. 2007. In: *Friction Stir Welding and Processing*. Chapter 5. 71-110.

[3] Nikolaos D. Alexopoulos, Evangelos Migklis, Antonis Stylianos, Dimitrios P. Myriounis. 2013. Fatigue behaviour of the aeronautical Al–Li (2198) aluminum alloy under constant amplitude loading. In: *International Journal of Fatigue 56*. 95-105.

[4] K. Krasnowski, C. Hamilton, S. Dymek. 2015. Influence of the tool shape and weld configuration on microstructure and mechanical properties of the Al 6082 alloy FSW joints. In: *Archives of Civil and Mechanical Engineering*. Volume 15. Issue 1. 133-141.

[5] S. Khan, O. Kintzel, J. Mosler. 2011. Experimental and numerical lifetime assessment of Al 2024 sheet. In: *International Journal of Fatigue*. Volume 37. 112-122.

[6] A. P. Reynolds, F. Duvall. 2009. Digital Image Correlation for Determination of Weld and Base Metal Constitutive Behavior. In: *Welding Research Supplement*. 355-360.

[7] ARAMIS Software. www.gom.com.